JOURNAL OF THERMOPHYSICS AND HEAT TRANSFER
Vol. 8, No. 3, July–Sept. 1994

Rapid Cooling by Direct Expansion of Coolant Through an Orifice

I. C. Hsu*
Lockheed Research and Development Division, Palo Alto, California 94301
and
J. H. Ambrose†
Lockheed Space Systems Division, Sunnyvale, California 94089

This article describes an experimental study of a novel rapid cooling scheme for sensor optics. The scheme involves direct expansion of a coolant from a high pressure to ambient conditions, resulting in a two-phase mixture with a high cooling capacity. Such a system is reliable, lightweight, and requires no servicing. Therefore it can provide significant weight, volume, and/or operational advantages over other expendable cooling schemes such as stored cryogens and conventional Joule-Thompson coolers. Results are presented which demonstrate the feasibility of this scheme for cooling the optics to temperatures of 180 K or less in less than 75 s. Various coolants were considered and the relative merits of these for rapid cooling are discussed.

Nomenclature

A = orifice flow area
g = gravitational acceleration
h_{fg} = latent heat of vaporization
$h_{\min}$ = film boiling heat transfer coefficient
k = vapor thermal conductivity
m = mass flow rate
P_b = downstream pressure
P_0 = upstream pressure
T = temperature
x_e = quality after expansion
$\Delta T_{\min}$ = Leidenfrost temperature difference
$\Delta\rho$ = liquid-vapor density difference
μ = kinematic viscosity
ν = dynamic viscosity
ρ_v = vapor density
ρ_l = liquid density
σ = surface tension coefficient

Introduction

VARIOUS terrestrial and space-borne Long Wavelength Infra-Red (LWIR) sensors require cold optics (<180 K) to reduce unwanted emission in the infrared wavelengths. If a sensor is functioning for only a short duration or is intended for intermittent operation, it may be desirable to cool the optics on demand. Significant system benefits can be realized if the optics can be rapidly cooled from ambient to operating temperature and maintained during sensing operations. In this case, a stored cryogen cooler, a mechanical cooler, or a cold radiator cooling system may be eliminated, reducing system weight and complexity. These methods may not be feasible for other reasons, such as availability of servicing, necessary power system, or a cold environment. This article describes results of an experimental investigation to demonstrate the feasibility of rapidly cooling sensor optics with a low mass expendable coolant system.

It is well known that when a fluid at high pressure is rapidly expanded through an orifice to a much lower pressure environment, the expansion occurs at constant enthalpy and the temperature of the fluid decreases due to the Joule-Thomson (J-T) cooling effect. J-T cooling will occur only when the temperature of the fluid upstream of the orifice is less than its inversion temperature. For the cooling of sensor optics, it was assumed that a 350-g aluminum mass [representing a lens housing and/or mirror(s)] was to be cooled from 300 K to below 180 K in approximately 75 s. The time requirement may vary with application, but a short cool-down period would generally be advantageous. Estimates of J-T cooling system mass were made for comparison with the direct expansion cooling concept and the results are summarized in Table 1. Some common J-T working fluids were considered with initial conditions of 300 K and final conditions corresponding to saturation at atmospheric pressure. An initial pressure was selected based on the thermodynamic properties of the fluid. Each of these systems results in ultimate temperatures substantially below 180 K. The J-T heat exchanger mass was estimated based on the calculated gas flow rates and existing J-T design data. Tank requirements were estimated from the gas supply volume and pressure. It was found that for the sensor optics cooling requirement, system masses were substantial. The lightest alternative is methane, however, methane gas will produce unwanted absorption in the LWIR.

Other fluids with higher critical temperatures may be expanded directly to a two-phase mixture without precooling. This eliminates the need for a J-T heat exchanger and speeds up the generation of a two-phase mixture. The proposed cooling concept is illustrated in Fig. 1. A coolant, initially at ambient temperature saturated conditions (or under proper supercritical conditions) is expanded directly through an orifice and flows into a plenum which is integral to the optical component. It then exhausts to the ambient environment through a suitable opening or tube. An exhaust pressure below 1 atm may be required to obtain substantial cooling below 180 K for the candidate coolants. However, a natural vacuum environment is always available to space-borne and high-altitude sensors.

The objective of this proof-of-concept experimental study is to demonstrate rapid cooling of sensor optics by direct

Presented as Paper 93-2858 at the AIAA 28th Thermophysics Conference, Orlando, FL, July 6–9, 1993; received Sept. 10, 1993; revision received Jan. 4, 1994; accepted for publication Jan. 5, 1994.

*Staff Scientist, Senior, Thermal Sciences Laboratory, M/S 9240 B205, Lockheed Palo Alto Research Labs., 3251 Hanover St. Member AIAA.

†Research Specialist; currently Spacecraft Thermodynamics Department, Space Systems Division, M/S 7411 B150, Lockheed Missiles and Space Co., Inc., P.O. Box 3504, Sunnyvale, CA 94089. Member AIAA.

Table 1 Estimated J-T cooling system parameters for 350-g optics

Parameter	Coolant methane	R14	Krypton	Argon	Nitrogen
Final temperature, K	120	150	130	95	80
Supply pressure, MPa	41.4	27.6	53.8	53.8	53.8
Coolant mass, g	259	543	988	1830	3276
System mass,[a] g	1487	1564	3242	5524	9096

[a]Includes coolant supply tank and J-T heat exchanger.

Table 2 Coolant properties, predicted cooling effect and system parameters

Parameter	Coolant ethane	Propane	R23	Krypton[a]
NBP, K	184.6	231.1	191.1	119.8
h_{fg}, J/g	491.1	427.8	241.8	107.6
x_e	0.74	0.39	0.62	0.93
Heat removal capability, J/g	128	261	92	8.1
Coolant mass, g	141	86	299	5,907
Average flow rate, g/s	1.9	1.1	4.0	78.8
Density, g/cc	0.36	0.49	0.75	1.47
Pressure, MPa	3.85	0.855	4.48	41.5
Tank volume, cc	393	175	299	4,018
Mass of tank plus coolant, g	546	267	607	10,046

[a]Initial conditions 50 Mpa.

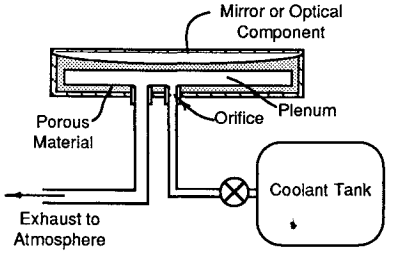

Fig. 1 Two-phase cooling concept for rapid cooling of optics.

expansion of a coolant through an orifice without a J-T heat exchanger. Another objective is to determine which coolants and design characteristics result in the best system performance, and which systems would be likely candidates for a particular set of sensor cooling requirements.

Selection of Coolant

A survey of common cooling fluids was performed to determine which can satisfy the thermal requirements for a rapidly cooled sensor system. The current concept was evaluated to verify weight advantages for the same requirements used above for the J-T cooling system. The system should have the lowest possible coolant/tank mass and should provide the minimum temperature in the shortest duration. It is generally necessary to terminate coolant flow prior to sensing operations to eliminate unwanted vibration effects.

The thermodynamic properties[1] of the fluids considered for direct expansion cooling are listed in Table 2, along with predicted quality x_e following isenthalpic expansion from 300 K to 1 atm. With the exception of krypton, the coolants are two-phase at the initial condition (R23 is slightly supercritical, TC = 299.1 K). Provided a sufficiently high supply pressure, krypton can be expanded directly to two-phase conditions. The two-phase cooling effect following expansion may be rated by the heat removal capability, defined as the liquid mass fraction $(1 - x_e)$ times the latent heat h_{fg}. These values are also listed in Table 2. Even though the normal boiling points of ethane, propane and R23 are all above 180 K, the temperature of the two-phase fluid can be reduced by vacuum pumping on the downstream side of the orifice. Therefore, the cooling effect and system mass predicted here is to be used for qualitative comparison only. The lower limit of the temperature that can be achieved by the expanded fluid downstream of the orifice is the triple point of the fluid, at which point it may solidify and plug up the orifice. Since the triple point pressure for the candidate fluids is much less than 0.1 atm, the triple point of the coolant will not likely be reached using the current scheme.

The required coolant mass and mass flow rates were estimated in order to determine approximate tank size and flow rate requirements for each of the candidate coolants. The mass of coolant required is based on the total heat that has to be removed. A sensor optics mass of 350 g of aluminum was assumed. The integrated energy removal was computed for each coolant for an initial temperature of 300 K and final conditions corresponding to saturated conditions at 1 atm (accounting for the variation in specific heat). Table 2 shows the estimated mass flow rates required to cool the optical components within 75 s for the four coolants. In addition, the tank size and mass required for storing each candidate coolant at ambient temperature were calculated for comparison. For the proof-of-concept experimental study, ethane, propane and R23 were selected as the candidate fluids based on the lower mass required as shown in Table 2.

Heat Transfer Performance

For the rapid cooling of optics, the requirements for the coolant are good wetting, high latent heat of vaporization and high vapor pressure. The heat transfer process is one of intense evaporation due to the impingement of a two-phase mixture. The process is exactly similar to evaporative spray cooling since the mixture will be a finely dispersed spray following expansion through the orifice. The heat transfer coefficients in evaporative spray cooling are typically high, and depend on spray characteristics such as liquid mass fraction, droplet size, and velocity.[2] All of the organic fluids discussed here should exhibit good wetting on clean metal surfaces. The large expansion ratio of the fluid will produce high flow velocities over a wide range of flow rates. Thus, the heat transfer rates will depend mainly upon the thermodynamic properties, namely the saturation temperature and quality following expansion through the orifice.

For the two-phase evaporation cooling process, the saturation temperature of the fluid following expansion is a function of the exhaust pressure and the working fluid. Because the working fluid must be exhausted through a duct to the atmosphere, there will exist a finite pressure drop between the plenum and the atmosphere. Although ambient pressures below 1 Torr may be common in applications, plenum pressures below 1 Torr are not practical during the cooldown phase due to the relatively high flow rates. Based on the saturation poperties, ethane and R23 will have similar limiting temperatures in the range of 120–150 K, and propane will be limited to temperatures of greater than 150 K.

The other parameter of major interest will be the flow quality, since it fixes the liquid mass fraction. The lowest quality will produce the highest initial heat transfer rates, since the heat removal capability (Table 2) will be highest. At a given mass flow rate, velocity will increase with increasing quality, but this is a second-order effect compared to the decrease in liquid fraction. Propane has high heat removal capability but will also have the highest saturation temperature.

Coolant Flow Modeling

The characteristics of the flow pattern will depend on the flow rate and the geometry of the flow passages. For the relatively high flow rates and complex geometries expected for rapid cooling of optical components, detailed modeling of the two-phase flow patterns is not practical. However, simplified calculations can provide some insight into the observed heat transfer results and suggest improved design concepts for the actual optical components.

Due to the rapid acceleration through the orifice, the coolant will enter the plenum as a high-velocity spray. It is desirable to have the maximum possible outlet quality to minimize the exhaust pressure drop and to collect and retain the maximum amount of liquid for continued cooling after termination of the flow. Liquid entrainment must therefore be minimized. It is possible to utilize porous material and properly designed outlet flow passages to accomplish this goal. The entrainment limit is determined from the ratio of capillary and inertia forces, characterized by the Weber number. Simple one-dimensional flow calculations were performed for the case of the primary mirror with coolant exhaust channels embedded in the wick structure. The flow was assumed to be R23 vapor ($x = 1$). In the actual article, a finite liquid fraction will always exist, resulting in substantially higher flow pressure drop, but lower velocities. For square exhaust passages of 3 mm separated by 3-mm wick elements, the results show that the flow velocities are in the range of 10–40 m/s during the blowdown phase and exhaust pressure drops are between 1–10 Torr. Assuming a Weber number of unity, the maximum pore size range is 20–30 μm to prohibit entrainment of liquid which has saturated the porous material.

For preliminary design calculations, the coolant flow rate through the orifice into the plenum was predicted using the procedure suggested by Fauske[3] for saturated liquids. For orifices, the conventional orifice discharge equation is used:

$$\dot{m} = 0.61 A_c \sqrt{2\rho_l (P_0 - P_b)} \tag{1}$$

The temperature and pressure of the supply tank is assumed to remain constant during the blowdown cooling process, and the pressure loss upstream of the orifice is assumed negligible. The mass flow rate predicted by Eq. (1) is shown in Fig. 2 along with R23 flow rates measured in cooldown tests for several orifice diameters. The R23 flow rates were obtained from cylinder weight measurements before and after each test run, and represent approximate average rates. The R23 was initially at room temperature saturated conditions and was expanded through the orifice into a vacuum with negligible downstream pressure. The poor agreement between predicted and measured values at higher flow rates is due to pressure losses upstream of the orifice and inlet quality greater than zero.

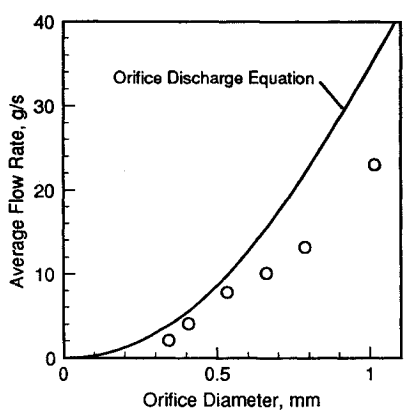

Fig. 2 Measured and predicted two-phase flow of R23 through an orifice.

Transient Thermal Model

Simplified transient thermal models were used to assess the effects of various parameters on the overall cooling performance. Both a lumped model and a one-dimensional numerical model were utilized. The lumped model results allow a simple evaluation of the heat transfer coefficients obtained in the tests. The lumped model was used to study the heat transfer and thermal mass effect. Depending upon the relative magnitude of the heat transfer coefficient and the thermal mass of the optics, the wetting phenomenon may or may not be apparent in the cooling curves as shown in Fig. 3 for a fixed ΔT_{min} of 10 K.

The numerical model allows evaluation of film boiling behavior and conduction in the wick. It assumes that heat is transferred between a single two-phase coolant heat sink and the wick; the wall is cooled by conduction to the wick. The convective heat transfer coefficient between the wick and the coolant corresponds to either spray evaporation or film boiling conditions, depending upon the Leidenfrost criterion. The spray evaporation heat transfer coefficient was estimated to be 2000–5000 W/m^2-K, based on available spray cooling data for Freon-113,[4] and screen-wick evaporation data for Freon-11 and 113.[5] This represents an order of magnitude estimate only, since the actual heat transfer coefficients will vary with exit quality, flow rate, and passage geometry.

Ignoring the sensible heat effect of the vapor layer, the film boiling coefficient may be estimated from[6]

$$h_{min} = 0.425 \left[\frac{k_l^3 \rho_v \Delta\rho g h_{fg}}{\mu_v \Delta T \sqrt{(\sigma/g\Delta\rho)}} \right]^{1/4} \tag{2}$$

where the properties in the brackets are evaluated at the mean film conditions, except for σ, $\Delta\rho$, and h_{fg}, which are saturated conditions. For R23 at 180 K, this yields a film boiling coefficient in the range of 5 W/m^2-K. Leidenfrost criteria may be estimated from the relationship of Berenson and Zuber[6]:

$$\Delta T_{min} = 0.127 \frac{\rho_v h_{fg}}{k_v} \left[\frac{\mu_v \Delta\rho g}{(\rho_l + \rho_v)^2} \right]^{1/3} \left(\frac{\sigma}{\Delta\rho g} \right)^{1/2} \tag{3}$$

For R23 at a saturation temperature of 180 K, this relationship yields a ΔT_{min} of about 9 K.

The numerical model was used to study the effect of Leidenfrost point and wick thermal conductivity. For ΔT_{min} greater than 10 K, a distinct wetting point was not observed for a two-phase heat transfer coefficient of 5000 W/m^2-K. For ΔT_{min} less than 10 K, cooling was slowed and a distinct wetting curve similar to those in Fig. 3 was obtained. The effect of wick thermal conductivity is shown in Fig. 4, assuming a heat transfer coefficient of 5000 W/m^2-K and ΔT_{min} of 10 K .

Experimental System

Various test articles were investigated as part of the experimental study, including a primary mirror, a mockup sec-

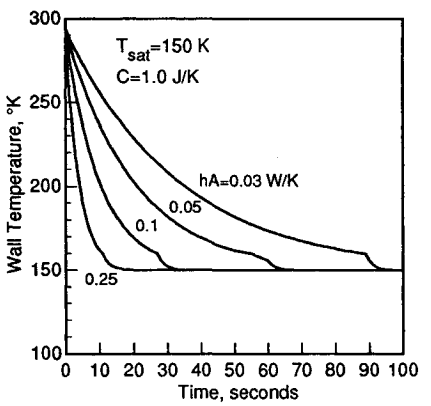

Fig. 3 Predicted cooling with differing relative heat transfer rates.

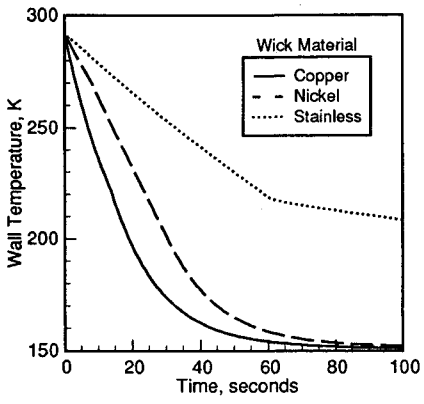

Fig. 4 Predicted cooling with differing wick thermal conductivities.

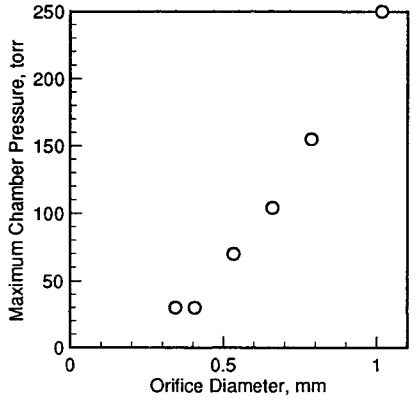

Fig. 6 Increase in chamber pressure with orifice size.

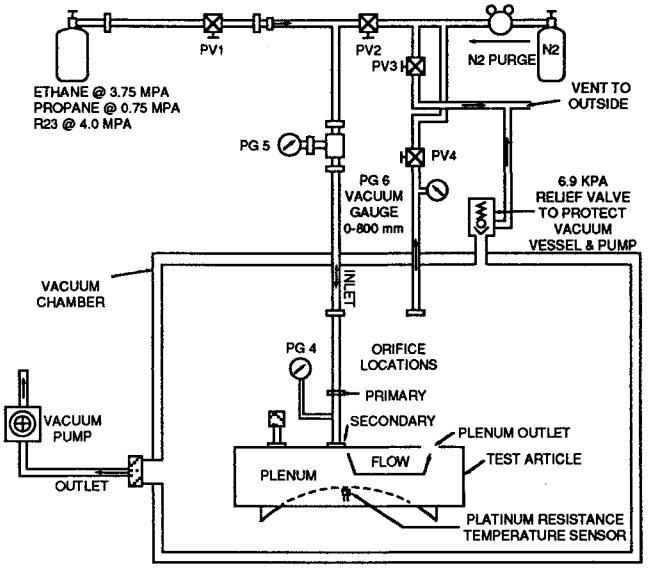

Fig. 5 Vacuum chamber configuration used for rapid cooling tests.

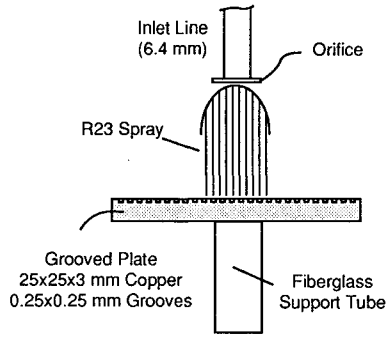

Fig. 7 Grooved plate test article configuration.

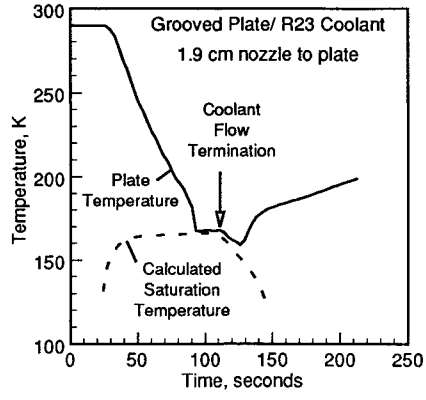

Fig. 8 Grooved plate test results.

ondary mirror, and a small grooved plate. Tests were performed in a small vacuum chamber equipped with feed-throughs for coolant lines and the necessary instrumentation. The chamber was used to minimize parasitic heat load and to prevent moisture from condensing on the test article surface. The test setup is shown in Fig. 5. For the primary mirror, tests were performed for expansion of coolant to either ambient pressure or subatmospheric pressure environments. Since ethane and propane are flammable fluids, a nitrogen purging system was incorporated into the test system to prevent any mixing of ethane or propane with oxygen from the ambient environment.

Chamber pressure measurements were obtained from a 0–1000 Torr transducer mounted to a fitting on the chamber. The estimated measurement accuracy for this measurement is $\pm 0.75\% + 0.5$ Torr. The supply pressure upstream of the orifice was measured with a 0–6.9-MPa transducer mounted in the coolant line. The estimated measurement accuracy for this measurement is $\pm 2\%$. Calibrated platinum resistance temperature-sensors (PRTs) were used for measurement of the test article temperatures. For all tests, the sensors were epoxy-bonded in the center of the outer face of the test article, opposite the coolant inlet. The accuracy of the temperature measurements was estimated as $\pm 2\%$ of the reading in °C. Two different vacuum pumps were utilized for evacuating the chamber and removing the coolant exhausted directly into the chamber. The pump capacity determined the lowest pressure which could be maintained for a given coolant and flow rate. A vacuum pump with a pumping capacity of 18.9 l/s was used for the primary mirror tests and most of the secondary mirror tests. The maximum chamber pressure for this pump increased with orifice size (flow rate) as shown in Fig. 6 for R23. A smaller pump was used for the grooved plate tests and the nickel-wicked secondary mirror tests. Coolant was supplied from either the vendor-supplied cylinder (inverted with valve downward) or dual 1-l cylinders plumbed in series with internal dip tubes to ensure low quality coolant supply. In either case, the coolant supply pressure was approximately constant in all tests.

Results

Grooved Plate

A small grooved copper plate was used to experimentally study the flash evaporation cooling with R23 in a vacuum environment. The plate was placed directly under a coolant nozzle formed by attaching a 0.34-mm orifice to the end of a tube and was supported by a small fiberglass tube as shown in Fig. 7. It was possible to visually observe the spray and the wetting process on the grooved plate through the vacuum chamber window. The wetted zone would begin near the center of the spray cone and progress outward as the temperature of the plate approached the saturation temperature. The high-velocity flowfield entrained most of the liquid in the spray

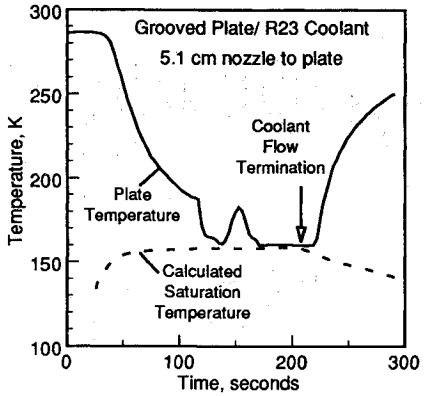

Fig. 9 Grooved plate test results—low flow.

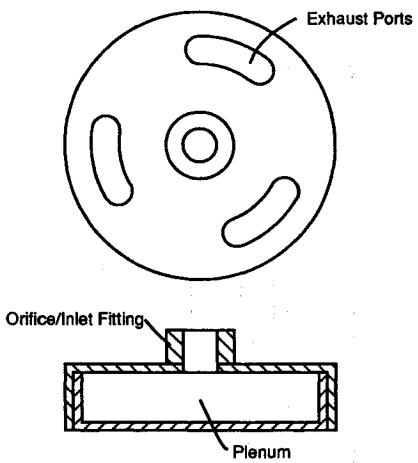

Fig. 10 POC secondary mirror test article.

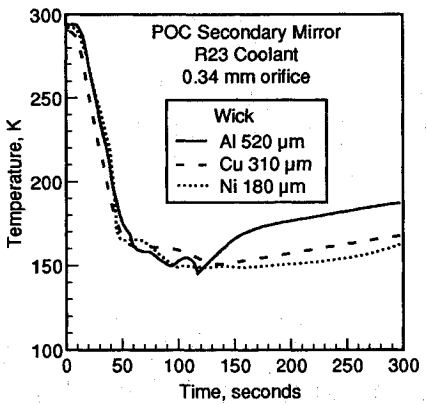

Fig. 11 POC secondary mirror test results.

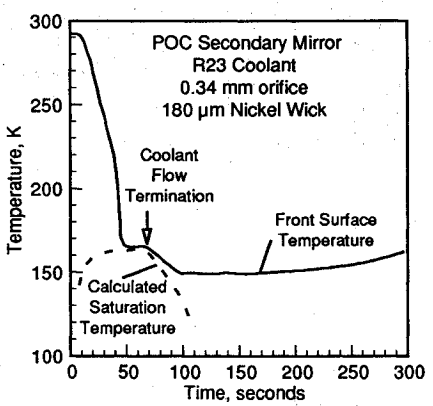

Fig. 12 POC secondary mirror test results.

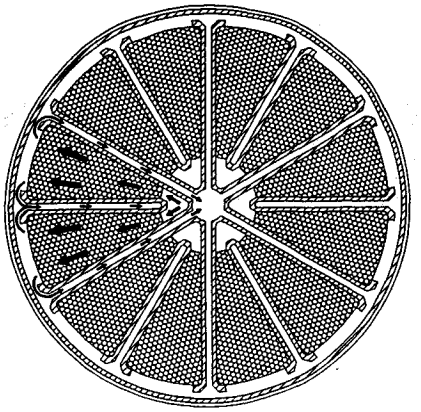

Fig. 13 Primary mirror flow geometry.

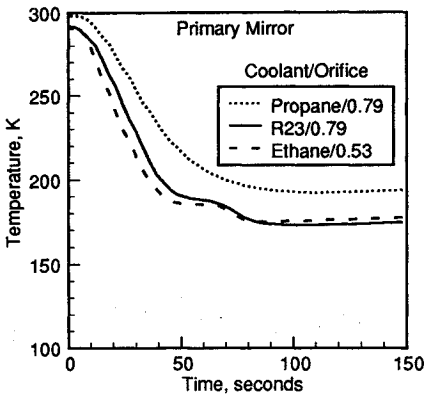

Fig. 14 Primary mirror test results—various coolants.

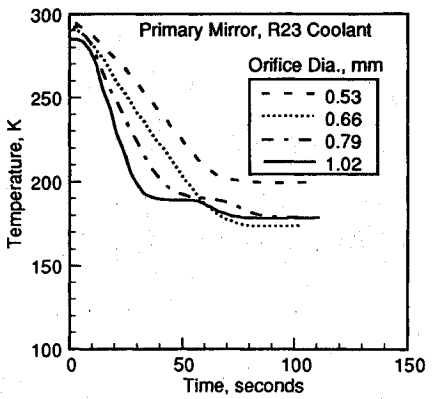

Fig. 15 Primary mirror test results—R23.

and left only a small streak of wetted area stretching to each side of the center point. The ultimate temperatures reached for these tests are in good agreement with the R23 saturation temperature based on measured chamber pressures. Representative results are shown in Fig. 8.

During some tests, the small orifice apparently became partially clogged with a foreign substance, as verified by the substantially lower flow rate and subsequent examination of the orifice. At the lower flow rate, the wetting process was much more pronounced due to the lower overall heat transfer coefficient as seen in Fig. 9. The observed Leidenfrost temperature difference is in fair agreement with predicted values.

Proof of Concept (POC) Secondary Mirror

Several secondary mirror blanks were constructed and tested to assess the effect of wick material, mass flow rate, and exhaust geometry. The configuration is shown in Fig. 10. The test article was constructed from aluminum and weighs 28 g without wick material. An integral fitting was used to mount

Table 3 Summary of cooling effectiveness for tests

Test article/wick[a]	Coolant	Orifice diameter, mm	Total cooling, J	Coolant mass, g	Cooling effect, J/g
SM/520 μm Al	R23	0.53	3,528	450	7.8
SM/310 μm Cu	R23	0.34	3,202	114	28
SM/180 μm Ni	R23	0.34	3,978	76	52
PM/1 mm Al	Ethane	0.53	35,640	318	112
PM/1 mm Al	Propane	0.79	30,700	227	135
PM/1 mm Al	R23	0.53	36,730	462	80
PM/1 mm Al	R23	0.66	43,080	600	72
PM/1 mm Al	R23	0.79	41,980	792	53
PM/1 mm Al	R23	1.02	43,060	1,380	31

[a]SM—Secondary mirror; PM—primary mirror.

the orifice. Coolant was exhausted through the small cutout vents directly into the test chamber.

The article was tested with different orifice sizes and internal wick materials. Typical results are shown in Fig. 11. The wick materials which were available for these tests had relatively large pore sizes (150–600 μm). However, the smallest pore materials did exhibit some retention of liquid based on the results. From the computed Weber numbers in the test article, a high degree of liquid entrainment is expected, and the percentage of liquid retention is small based on the calculated parasitic heat leak and the observed cooling effect. The temperatures obtained in the tests with the top exhausts (aluminum and copper wicks) did not closely match the saturation temperature corresponding to the measured chamber pressures. The difference in predicted saturation pressure is due to the pressure drop in the coolant outlet. The test article was modified for the nickel wick so that coolant exhausted through slots on the side. Good agreement between R23 saturation temperature at measured chamber pressures and minimum mirror temperatures was obtained as shown in Fig. 12.

Primary Mirror

The primary mirror used for this study weighed approximately 350 g. It has an internal flow passage geometry as shown in Fig. 13. This passage geometry was configured to meet a specific cooling technique/requirement as described in an earlier study.[7] The passages have a relatively open foam material (pore size about 1 mm) in the coolant plenum. Coolant must flow through the channels and the foam material to reach the exhaust.

Test results were obtained for rapid cooling of the primary mirror using ethane, propane, and R23 as coolants. Results are summarized for direct expansion of the three coolants through various sizes of orifices in Fig. 14. The lowest temperature reached by the mirror within 75 s of coolant flow initiation was 178 K, achieved by using ethane as the coolant with an orifice diameter of 0.53 mm. Overall, ethane has the best results, cooling the mirror to the lowest temperature while requiring a lower mass flow rate. As the coolant flows through the cooling channels and exhausts into the vacuum chamber, its pressure continuously decreases until it reaches the chamber pressure at the exhaust. This was verified by pressure measurements immediately downstream of the orifice, which showed a pressure substantially higher than the chamber pressure. The saturation temperature corresponding to the two pressures (upstream of orifice and chamber) in all cases bounded the observed minimum mirror temperatures, as expected. For all the test runs, after the flow of coolant was terminated, the temperature of the mirror decreased before increasing again due to retained liquid coolant.

Cooldown rates were measured as a function of orifice size for R23 coolant and the results are shown in Fig. 15. As the size of the orifice and mass flow rate decrease, the cooldown time for the mirror increases due to the lower heat transfer coefficient. The limiting temperature also decreases due to the lower chamber pressure and coolant saturation temperature.

Summary of Results

The observed cooling for each test article was calculated based on the initial and final temperatures and the thermal mass. This quantity divided by the total mass of coolant consumed yields a cooling effect for the process, shown in Table 3. As expected, the values are always less than the heat removal capability shown in Table 2. For the primary mirror, at lower relative flow rates, the theoretical cooling capability value is approached.

Conclusions

Rapid cooling by direct expansion of coolant through an orifice has been demonstrated in a series of tests using ethane, propane, and R23. The lowest temperature reached by the aluminum primary mirror after 75 s of cooling was 178 K for ethane with an 0.53-mm diam orifice. R23 and ethane both yield similar performance, yielding minimum temperatures of about 160–180 K following termination of coolant flow. The primary mirror internal geometry was not designed for collection and retention of liquid coolant, and the performance could be significantly enhanced. Ultimate temperatures of less than 150 K were demonstrated for the smaller secondary mirror using R23. Based on the secondary mirror results with various wick properties, a substantial retention of liquid can be obtained to further cool the mirror following coolant flow termination. Coupling this feature with proper design of the exhaust passages, temperatures approaching the triple point of the coolants may be reached by flash evaporation following coolant inlet flow termination. By optimizing the design of the mirrors and other optical components, a lightweight system without a Joule-Thomson heat exchanger can be designed for cooling of sensor optics.

References

[1]*ASHRAE Handbook 1981 Fundamentals*, American Society of Heating, Refrigerating and Air-Conditioning Engineers, Inc., Atlanta, GA, 1981.

[2]Tilton, D. E., Pais, M. R., and Chow, L. C., "High Power Density Spray Cooling," Wright Research and Development Center, WRDC-TR-89-2082, July 1989.

[3]Fauske, H. K., "The Discharge of Saturated Water Through Tubes," *Chemical Engineering Progress Symposium Series*, Vol. 61, No. 59, 1965, pp. 210–216.

[4]Holman, J. P., and Ghodbane, M., "Experimental Study of Droplet Heat Transfer Suitable for Cooling of Electronic Equipment," Wright Research and Development Center, WRDC-TR-89-2020, May 1989.

[5]Rannenberg, M., and Beer, H., "Heat Transfer by Evaporation in Capillary Porous Wire Mesh Structures," *Letters in Heat and Mass Transfer*, Vol. 7, No. 6, 1980, pp. 425–436.

[6]Rohsenow, W. M., "Boiling," *Handbook of Heat Transfer*, edited by W. M. Rohsenow and J. P. Hartnett, McGraw-Hill, New York, 1973, pp. 13-1–13-75.

[7]Hsu, I., and Plummer, R., "Thermal Design and Analysis for a Rapidly Cooled Beryllium Mirror," AIAA Paper 92-2842, July 1992.